University of Nebraska - Lincoln

DigitalCommons@University of Nebraska - Lincoln

10-31-2013

Electric Control of Exchange Bias Training

W. Echtenkamp
University of Nebraska-Lincoln

Christian Binek
University of Nebraska-Lincoln, cbinek@unl.edu

Electric Control of Exchange Bias Training

W. Echtenkamp and Ch. Binek*

*Department of Physics and Astronomy and Nebraska Center for Materials and Nanoscience, University of Nebraska,
Lincoln, Nebraska 68588-0111, USA*
(Received 13 June 2013; published 31 October 2013)

Voltage-controlled exchange bias training and tunability are introduced. Isothermal voltage pulses are used to reverse the antiferromagnetic order parameter of magnetoelectric Cr_2O_3, and thus continuously tune the exchange bias of an adjacent CoPd film. Voltage-controlled exchange bias training is initialized by tuning the antiferromagnetic interface into a nonequilibrium state incommensurate with the underlying bulk. Interpretation of these hitherto unreported effects contributes to new understanding in electrically controlled magnetism.

Voltage-controlled exchange bias is a seminal achievement in nanomagnetism. It enables dissipationless electric control of interface magnetic states and is an example of electric control of magnetism [1–4]. Exchange bias can emerge at the interface of adjacent ferromagnetic (FM) and antiferromagnetic (AFM) thin films through quantum mechanical exchange interaction. The interlayer exchange creates unidirectional anisotropy in the FM layer. This alters its magnetization reversal manifested in a shift of the FM hysteresis loop along the magnetic field axis by an amount H_{EB}, known as the exchange bias field. Voltage-controlled exchange bias is a recent achievement which refers to isothermal switching of H_{EB} in the absence of dissipative electric currents [3,4]. It promises significant implications for a new generation of spintronic applications such as ultralow power nonvolatile magnetic random access memories [5–7]. Exchange bias training refers to the change of the exchange bias field when cycling the FM layer through consecutive magnetic hysteresis loops. In the present study we extend our previous pioneering results on isothermal voltage-controlled switching of exchange bias by showing how intermediate bias values can be observed and how fundamental insight into interface magnetic properties can be obtained through training effects studies.

We investigate voltage-controlled exchange bias and exchange bias training in a perpendicular anisotropic heterostructure $Cr_2O_3(0001)/Pd_{0.5\ nm}/(Co_{0.6\ nm}Pd_{1.0\ nm})_3$. The FM CoPd multilayer has been grown by molecular beam epitaxy on the (0001) surface of a Cr_2O_3 (chromia) single crystal. Our experiments employ the same exchange bias heterostructure which helped to pioneer the isothermal voltage-controlled switching of exchange bias near room temperature [3]. Details about growth and structural characterization are outlined in Ref. [3].

Prior to measurement the chromia pinning system is prepared in a single domain state through magnetoelectric annealing [8] from 350 K to $T = 303\ K < T_N(Cr_2O_3) \approx 307\ K$, in perpendicular electric and magnetic fields of $E = 100\ kV/m$ and $\mu_0 H = 100\ mT$. Magnetic hysteresis

loops of the CoPd film are measured via the polar Kerr effect using the polarization modulation technique and phase sensitive detection outlined in Ref. [9].

Figure 1(a) shows a CoPd hysteresis loop with positive exchange bias measured at $T = 303\ K$ after magnetoelectric annealing. Figure 1(a′) shows the FM hysteresis loop with negative exchange bias after isothermal switching of the exchange bias through inversion of the E field while maintaining a positive magnetic field of $\mu_0 H = 100\ mT$. Figure 1(b) shows details of the complete hysteretic switching. In depth resolution is shown at the transition; here intermediate states prone to exchange bias training are electrically set and probed by the intermediate equilibrium
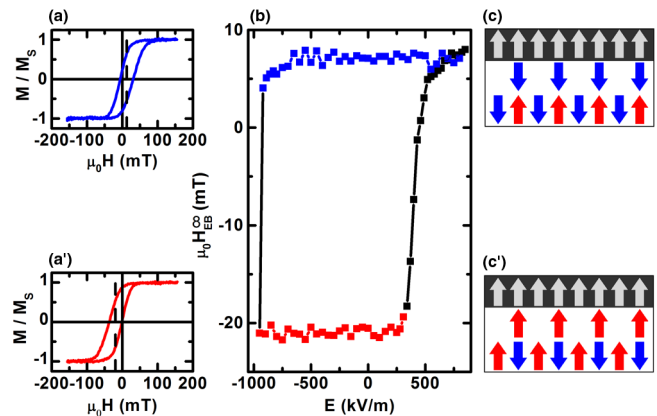

FIG. 1 (color online).   (a) Hysteresis loop of pinned CoPd thin film after magnetoelectric annealing of the sample. The dashed line illustrates positive exchange bias. (a′) Hysteresis loop of pinned CoPd thin film after electrically switching the spin configuration of chromia. The dashed line illustrates negative exchange bias. (b) Hysteretic behavior of equilibrium exchange bias with respect to applied electric field, a constant magnetic field of 100 mT is simultaneously applied. (c) Diagrams of the spin structure (up and down arrows) of the AFM bulk (bottom layer), FM boundary magnetization at the AFM interface (middle layer), and FM spins (top layer) in the positive exchange bias state (c), and in the negative exchange bias state (c′).

exchange bias fields, $\mu_0 H_{EB}^{\infty}$. Reversing E at constant H can switch between AFM single domain states. The two single domain spin structures presented in Fig. 1(c) correspond to those two saturation regions of the hysteresis loop presented in Fig. 1(b). The spin structure of the bulk (bottom layer), the boundary magnetization at the AFM interface (middle layer), and the ferromagnet (top layer) is shown. The positive and negative boundary magnetization switches together with the voltage-controlled reversal of the bulk AFM order parameter. Consequently, the exchange bias fields switch as shown in Fig. 1(a).

In this Letter we introduce electric control of exchange bias training. We demonstrate electric control of the degree of training between zero and large training effects which include an unusual crossover from negative to positive exchange bias fields. Electric control of exchange bias training is accompanied by tuned equilibrium exchange bias fields, $H_{EB}^{\infty} = H_{EB}(n \rightarrow \infty)$. They are the asymptotic stationary values after a large number n of training cycles. Our data show that both the tuning and the training effect are caused by boundary magnetization of the magnetoelectric antiferromagnet, which can either be commensurate or incommensurate with the underlying bulk.

A remarkable property of magnetoelectric AFM-FM exchange bias heterostructures is the possibility to select states where training is completely absent. This is achieved, for example, when the AFM pinning system is in one of its degenerate AFM single domain states [3]. In the magnetoelectric antiferromagnet Cr_2O_3 (chromia), a single domain state can be selected either thermally assisted via magnetoelectric annealing or isothermally through application of overcritical values of combined electric and magnetic fields, $|EH| > |EH|_c$ [2,10,11]. Exchange bias training requires pinning systems to be out of equilibrium. Relaxation is triggered in discrete steps on subsequent cycles of the FM hysteresis [12]. This model has been confirmed for remarkably diverse classes of magnetic heterostructures and nanoparticle systems such as exchange bias in graphene nanoribbons, hard layer-soft layer ferromagnetic films, and FM–spin-glass heterostructures [13–15].

We show that magnetoelectric antiferromagnets provide an exceptionally simple way to electrically control the AFM order parameter η and to bring the boundary magnetization out of equilibrium. Isothermal voltage control allows us to set η in the range $-1 \leq \eta(E) \leq 1$. We utilize $H_{EB}^{\infty}(E)$ to probe voltage-selected AFM domain states with $|\eta(E)| < 1$. Conventional isothermal tuning of an order parameter requires control over the conjugate field. In the case of an antiferromagnet the conjugate field is h_{st}, the staggered field. It changes sign along with the periodicity of the AFM sublattice magnetization. Its experimental control is virtually impossible with a few exceptions such as artificial model systems realized by ultracold atoms in an optical lattice [16].

The situation is more favorable in magnetoelectric antiferromagnets. Here, magnetoelectric coupling allows switching of η in complete analogy to the first-order transition induced by h_{st} [17,18]. An applied electric field E can induce this first-order phase transition when a constant magnetic field H is simultaneously present. On approaching the critical threshold $(EH)_c$, the antiferromagnet transitions from $\eta = -1$ to $\eta = 1$ or vice versa through a sequence of domain states with $|\eta| < 1$. Here EH (or E if H is kept constant) is a control parameter analogous to h_{st} [3,10].

Only a few elaborate experimental techniques such as neutron scattering, x-ray magnetic linear dichroism, and second harmonic light generation allow measuring η directly [19–21]. We use the exchange bias field to quantify transitional domain states during electric switching of η. The approach relies on the experimentally confirmed concept that H_{EB} depends linearly on the pinned AFM interface magnetization [22–24]. In magnetoelectric antiferromagnets this interface magnetization has a unique origin. Here the symmetry conditions are such that roughness insensitive boundary magnetization, m_{BM}, emerges. m_{BM} is intimately coupled to η [25]. For chromia, m_{BM} emerges as an equilibrium net magnetic moment at the surface or interface [25–27].

In chromia, boundary magnetization is fully established at the (0001) surface in both of its two degenerate single domain states. Sizable m_{BM} pins an adjacent FM film via exchange interaction giving rise to exchange bias. The boundary magnetization is directly linked to η, with $|m_{EB}|$ at maximum for $|\eta| = 1$ and $m_{BM} = 0$ for $\eta = 0$. As a consequence, in equilibrium, $H_{EB}(E) \propto m_{BM}[\eta(E)]$ follows the isothermal switch of $\eta(E)$. Similarly, the temperature dependence $H_{EB}(T)$ follows the critical behavior of $\eta(T)$ on approaching T_N. Both experimental facts establish the approach to probe $\eta(E)$ via $H_{EB}^{\infty}(E)$ [3,25].

Figure 2(a) displays the hysteresis loop, $\mu_0 H_{EB}$ vs E, including the initial and equilibrium exchange bias fields near the switching transition. The initial exchange bias field is set via a voltage-pulse applied after the previous training cycle reached equilibrium. The exchange bias of the first loop, $H_{EB}(E, n = 1)$ (solid symbols), and the fifteenth loop $H_{EB}(E, n = 15) \approx H_{EB}^{\infty}(E)$ (open symbols) are plotted. The change in E between subsequent training cycles is small (30 kV/m per step), keeping the exchange bias training of each cycle small. In Fig. 2(b) the E field was abruptly changed from 300 to 526 kV/m resulting in large exchange bias training. In the latter case $H_{EB}(E, n)$ is plotted for $n = 1, 2,...,15$ in Fig. 2(c) (circles). Additionally, Fig. 2(c) (squares) shows three training sequences with less training effect. The data are taken after the smaller electric field steps of 30 kV/m corresponding to the hysteresis in Fig. 2(a). Note that during training cycles the E field is switched off.

The training of the exchange bias field toward $H_{EB}^{\infty}(E)$ does not imply that the bulk chromia relaxes
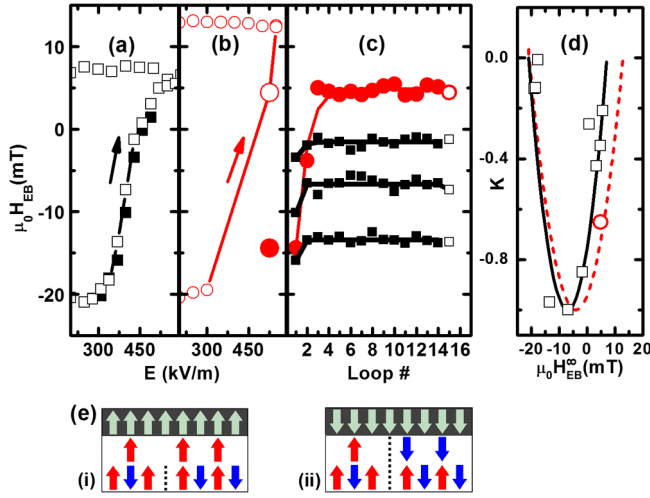
FIG. 2 (color online). (a) Example of the hysteretic behavior of exchange bias with respect to the electric field applied in steps of 30 kV/m. The initial exchange bias is illustrated with solid symbols and the equilibrium exchange bias is illustrated with open symbols. The arrow indicates the history of the measurements. (b) Example of the hysteretic behavior of exchange bias with respect to the applied electric field with one large step of 226 kV/m. The resulting initial and equilibrium exchange bias fields are displayed by large solid and open circles. The arrow indicates the history of measurements. (c) Circles show the exchange bias training series after initialization in a step from $E = 300$ to $E = 526$ kV/m. The first and fifteenth exchange bias values are also illustrated in (b) by a closed ($n = 1$) and open circle ($n = 15$), respectively. Squares show three exchange training series after initialization in a step from $E = 340$ to $E = 370$ kV/m, from $E = 370$ to $E = 400$ kV/m, and from $E = 400$ to $E = 430$ kV/m, respectively from bottom to top. First and fifteenth exchange bias values can be found in (a). (d) K vs $H_{EB}^{\infty}(E)$ for the training events arising from best fits of Eq. (1) to various training series corresponding to the squares in (a) and circles in (b). Solid and dashed lines are plots of Eq. (2) using $H_{EB}^{max/min}$ from the saturation values in (a) and (b). (e) Diagram of the spin structure (up and down arrows) in a domain state after electric field initialization before training (i), and in equilibrium (ii). The dashed line separates two domains with opposite order parameter.

asymptotically toward a single domain state. Bulk AFM domain states with $|\eta| < 1$ are metastable but energetically separated by pronounced local minima. This leaves the spin structure in the AFM bulk stationary in response to FM hysteresis loops of the CoPd layer. Initially, however, after applying the set fields, an AFM interface region, which determines the boundary magnetization, can deviate from a spin structure commensurate with the bulk. This mismatch originates from competing exchange with the underlying spins of the AFM bulk and exchange with the adjacent ferromagnet. Hysteresis loops of the FM film trigger relaxation of the AFM interface spin structure through coupling via m_{BM}. Consequently, the interface AFM spin structure relaxes toward an equilibrium state which

asymptotically becomes commensurate with the bulk. The changing m_{BM} accompanying the evolving AFM interface spin structure gives rise to training of H_{EB} towards $H_{EB}^{\infty}(E)$. The data in Fig. 2(a) show that equilibrium exchange bias can have any value between the saturation extremes. The absence of training in the differing saturation regions of the two $H_{EB}^{\infty}(E)$ loops presented in Figs. 2(a) and 2(b) strongly supports that exchange bias training originates from the interface region rather than the AFM bulk.

It is important to recognize that the initial exchange bias field $H_{EB}(E, n = 1)$ is not a unique function of EH but depends on the history as expected from a hysteretic effect. Specifically, $H_{EB}(E, n = 1)$ depends on the domain state of the AFM pinning layer before applying the set-fields. The history dependence explains the particularly pronounced exchange bias training shown in Fig. 2(c) (circles) which corresponds to the large solid ($n = 1$) and open ($n = 15$) circles highlighted in Fig. 2(b). Here initialization of $H_{EB}(E, n = 1)$ took place from the single domain state with $\eta = +1$. Intuitively, it is reasonable that the sizable electrically induced change from a single domain into a multidomain state drives the AFM interface far from equilibrium and thus far from a commensurate matching between interface and bulk. Figure 2(e) (i, ii) illustrate this process. The FM layer is kept in positive saturation during initialization of exchange bias training and stabilizes the positive boundary magnetization associated with negative exchange bias. The voltage-induced reversal of the majority of the AFM order parameter is depicted by splitting the bottom layer into two opposite domain states separated by a dashed line. The majority of the AFM bulk now favors negative boundary magnetization with positive exchange bias in equilibrium. This results in competition and non-equilibrium spin structure at the interface. Reversal of the FM layer (ii) triggers relaxation of the AFM interface spins accompanied by a large exchange bias training and a rather peculiar change in sign from $H_{EB}(E, n = 1) = -14.1$ mT to $H_{EB}(E, n = 15) = +4.43$ mT. The AFM bulk domain state is static in this process. Exchange bias training proceeds unidirectionally towards more positive values on the right side of the hysteresis and not necessarily towards the nearest single domain state. This behavior is inconsistent with bulk training, but fits well with exchange bias training due to competing exchange interactions at the interface. Note also that sizable exchange bias training can only be initialized at the right side of the $H_{EB}^{\infty}(E)$ hysteresis supporting the notion that exchange bias training requires competing interface exchange interactions. On the left side of the $H_{EB}^{\infty}(E)$ hysteresis the E field reverses the AFM order parameter into states favoring positive boundary magnetization. Positive boundary magnetization is, however, favored through exchange with the positively saturated FM film. Hence competition leading to incommensurate interface spin structures and thus exchange bias training are absent.

Next analysis of the exchange bias training is outlined with the help of the discretized Landau-Khalatnikov approach. This phenomenological approach is broadly applicable to a large number of effects with widely varying microscopic origins including magnetic and nonmagnetic relaxations. The theory has been developed previously for conventional AFM and FM pinning layers [12,14].

For magnetoelectric AFM-FM heterostructures the Landau-Khalatnikov theory of exchange bias training is analogous to training in the FM hard-soft bilayer. The formal correspondence originates from the fact that $m_{BM} \propto \eta$ just as the FM interface magnetization of a hard layer is proportional to the FM order parameter. The Landau-Khalatnikov theory for this scenario has been outlined in Ref. [14]. The explicit expression for the n dependence of the exchange bias field is obtained from the implicit sequence $H_{EB}(n+1) = (K+1)H_{EB}(n) - K H_{EB}^{\infty}$ and reads [14]

$$
H_{EB}(n) = (K+1)^{n-1}\Bigg\{ H_{EB}(n=1)
$$
$$
- KH_{EB}^{\infty}\left[\frac{(K+1)^{n+1}-1}{K(K+1)^{n-1}} - (K+2)\right]\Bigg\}. \quad (1)
$$

Figure 2(c) (circles) shows the full training sequence at $E = +526$ kV/m. The solid line shows a least squares fit of Eq. (1) to the data which yields a value of $K = -0.65$. The intuitive meaning of $-1 < K < 0$ is discussed in Ref. [28]. $K = -1$ is the extreme case of a steplike exchange bias training where H_{EB}^{∞} is reached for $n \geq 2$. $K \to 0$ resembles continuous training with small changes (zero change for $K = 0$). Based on Landau theory it has been shown that K is related to the 2nd order derivative of the free energy at the equilibrium point [28]. This translates here into $K \propto a + 3bm_{BM,eq}^2$ where $a < 0$ and $b > 0$ are the 2nd and 4th order coefficients of the Landau free-energy expansion in the symmetry broken phase and $m_{BM,eq}$ is the boundary magnetization in equilibrium. Using $H_{EB}^{\infty}(E) \propto m_{BM,eq}$ we expect that K and $H_{EB}^{\infty}(E)$ are related by a simple functional form of the type $K \propto a + \tilde{b}[H_{EB}^{\infty}(E)]^2$ with $a < 0$ and $\tilde{b} > 0$. Inspection of Figs. 2(a) and 2(b) shows that the saturation values H_{EB}^{max} and H_{EB}^{min} of the $H_{EB}^{\infty}(E)$ hysteresis differ in magnitude indicating that exchange bias training can be virtually zero even if full saturation of $m_{BM,eq}$ and η are not reached. We take the shift of the $H_{EB}^{\infty}(E)$ hysteresis with respect to zero exchange bias into account by modifying the K expression into $K \propto a + \tilde{b}(H_{EB}^{\infty}(E) + S)^2$. All of the free parameters in this expression can be eliminated utilizing the constraints $K(H_{EB}^{max}) = K(H_{EB}^{min}) = 0$ (no training) and $K_{min} = -1$ following from the convergence criterion of Eq. (1) [14]. The parameter-free $K(H_{EB}^{\infty}(E))$ function reads finally

$$
K = -1 + 4\left(\frac{H_{EB}^{\infty}(E) - \frac{1}{2}(H_{EB}^{max} + H_{EB}^{min})}{H_{EB}^{max} - H_{EB}^{min}}\right)^2. \quad (2)
$$

Figure 2(d) shows the experimental data K vs $H_{EB}^{\infty}(E)$ (squares) and a plot of Eq. (2) (solid line) with values H_{EB}^{max} and H_{EB}^{min} adapted from the solid hysteresis loop shown in Fig. 2(a). Likewise we compare Eq. (2), using H_{EB}^{max}, H_{EB}^{min} from the hysteresis loop in Fig. 2(b), with the data point, $K = -0.65$, resulting from the fit to the training data shown in Fig. 2(c) (circles). In both cases there is reasonable agreement with the theory confirming the microscopic model of the voltage-controlled exchange bias training as outlined above.

In conclusion, two new phenomena in electrically controlled magnetism have been introduced. These are the isothermal voltage-control of exchange bias training and the isothermal voltage-controlled gradual tuning of equilibrium exchange bias. These hitherto unreported effects are potentially useful additions to the family of voltage-controlled exchange bias phenomena. A gradually electrically tunable exchange bias field can add functionality to potential spintronic devices and thus has technological advantages over a recently reported binary switching [3]. The electrically controlled training effect can serve as a model example in nonequilibrium thermodynamics. Finally, it is emphasized that magnetoelectric antiferromagnets provide a simple way to electrically induce first-order reversal of the antiferromagnetic order parameter in the absence of an applied conjugate field.

*cbinek@unl.edu
 [1] A. Hochstrat, C. Binek, X. Chen, and W. Kleemann, J. Magn. Magn. Mater. **272–276**, 325 (2004).
 [2] P. Borisov, A. Hochstrat, X. Chen, W. Kleemann, and C. Binek, Phys. Rev. Lett. **94**, 117203 (2005).
 [3] X. He, Y. Wang, N. Wu, A. N. Caruso, E. Vescovo, K. D. Belashchenko, P. A. Dowben, and C. Binek, Nat. Mater. **9**, 579 (2010).
 [4] S. M. Wu, S. A. Cybart, D. Yi, J. M. Parker, R. Ramesh, and R. C. Dynes, Phys. Rev. Lett. **110**, 067202 (2013).
 [5] C. Binek and B. Doudin, J. Phys. Condens. Matter **17**, L39 (2005).
 [6] E. Y. Tsymbal, Nat. Mater. **11**, 12 (2012).
 [7] C. Binek, Physics **6**, 13 (2013).
 [8] T. H. O'Dell, *The Electrodynamics of Magneto-Electric Media* (North-Holland, Amsterdam, 1970).
 [9] S. Polisetty, J. Scheffler, S. Sahoo, Y. Wang, T. Mukherjee, X. He, and C. Binek, Rev. Sci. Instrum. **79**, 055107 (2008).
[10] P. Borisov, A. Hochstrat, X. Chen, and W. Kleemann, Phase Transit. **79**, 1123 (2006).
[11] T. J. Martin and J. C. Anderson, IEEE Trans. Magn. **2**, 446 (1966).
[12] C. Binek, Phys. Rev. B **70**, 014421 (2004).

[13] S. N. Jammalamadaka, S. S. Rao, J. Vanacken, V. V. Moshchalkov, W. Lu, and J. M. Tour, Appl. Phys. Lett. **101,** 142402 (2012).

[14] C. Binek, S. Polisetty, X. He, and A. Berger, Phys. Rev. Lett. **96,** 067201 (2006).

[15] S. Sabyasachi, M. Patra, S. Majumdar, S. Giri, S. Das, V. S. Amaral, O. Iglesias, W. Borghols, and T. Chatterji, Phys. Rev. B **86,** 104416 (2012).

[16] H. Zhang, Q. Guo, Z. Ma, and X. Chen, Phys. Rev. A **87,** 043625 (2013).

[17] M. E. Fisher and A. N. Berker, Phys. Rev. B **26,** 2507 (1982).

[18] K. Binder, Rep. Prog. Phys. **50,** 783 (1987).

[19] C. Binek, D. Bertrand, L. P. Regnault, and W. Kleemann, Phys. Rev. B **54,** 9015 (1996).

[20] J. Wu *et al.*, Nat. Phys. **7,** 303 (2011).

[21] M. Fiebig, D. Fröhlich, B. B. Krichevtsov, and R. V. Pisarev, Phys. Rev. Lett. **73,** 2127 (1994).

[22] H. Ohldag, A. Scholl, F. Nolting, E. Arenholz, S. Maat, A. Young, M. Carey, and J. Stöhr, Phys. Rev. Lett. **91,** 017203 (2003).

[23] A. Hochstrat, C. Binek, and W. Kleemann, Phys. Rev. B **66,** 092409 (2002).

[24] S. R. Ali, M. R. Ghadimi, M. Fecioru-Morariu, B. Beschoten, and G. Güntherodt, Phys. Rev. B **85,** 012404 (2012).

[25] K. D. Belashchenko, Phys. Rev. Lett. **105,** 147204 (2010).

[26] A. F. Andreev, JETP Lett. **63,** 758 (1996).

[27] N. Wu, Xi He, A. L. Wysocki, U. Lanke, T. Komesu, K. D. Belashchenko, C. Binek, and P. A. Dowben, Phys. Rev. Lett. **106,** 087202 (2011).

[28] S. Polisetty, S. Sahoo, A. Berger, and C. Binek, Phys. Rev. B **78,** 184426 (2008).